

<b>REPORT DOCUMENTATION PAGE</b>				Form Approved OMB No. 0704-0188	
<p>The public reporting burden for this collection of information is estimated to average 1 hour per response, including the time for reviewing instructions, searching existing data sources, gathering and maintaining the data needed, and completing and reviewing the collection of information. Send comments regarding this burden estimate or any other aspect of this collection of information, including suggestions for reducing the burden, to the Department of Defense, Executive Service Directorate (0704-0188). Respondents should be aware that notwithstanding any other provision of law, no person shall be subject to any penalty for failing to comply with a collection of information if it does not display a currently valid OMB control number.</p> <p><b>PLEASE DO NOT RETURN YOUR FORM TO THE ABOVE ORGANIZATION.</b></p>					
1. REPORT DATE (DD-MM-YYYY) 30-07-2013		2. REPORT TYPE FINAL		3. DATES COVERED (From - To) 01-05-2012 - 30-04-2013	
4. TITLE AND SUBTITLE Engineering Electronic and Optical Properties of Color Centers in Diamond				5a. CONTRACT NUMBER FA9550-12-1-0214	
				5b. GRANT NUMBER	
				5c. PROGRAM ELEMENT NUMBER	
6. AUTHOR(S) Maze, Jeronimo				5d. PROJECT NUMBER	
				5e. TASK NUMBER	
				5f. WORK UNIT NUMBER	
7. PERFORMING ORGANIZATION NAME(S) AND ADDRESS(ES) Pontificia Universidad Catolica de Chile, Av. Vicuna Mackenna 4860, Santiago 7820436, Chile				8. PERFORMING ORGANIZATION REPORT NUMBER  DUNS 980870054	
9. SPONSORING/MONITORING AGENCY NAME(S) AND ADDRESS(ES) Pontificia Universidad Catolica de Chile, Av. Vicuna Mackenna 4860, Santiago 7820436, Chile  AFRL				10. SPONSOR/MONITOR'S ACRONYM(S)  PUC	
				11. SPONSOR/MONITOR'S REPORT NUMBER(S)	
12. DISTRIBUTION/AVAILABILITY STATEMENT  Distribution A: Approved for public release					
13. SUPPLEMENTARY NOTES					
14. ABSTRACT  We report on the results achieved during the period of the proposal as well as the current progress that will lead to results outside this period. The work of the proposal has concentrated on controlling the electronic, optical and spintronics properties of color centers in diamond and their environment. A high level of control of the before mentioned properties is crucial to develop novel applications such as single photon sources on demand, high precision and high resolution magnetic and electric sensors and opto-electronic devices at very low power consumption. All these applications require a deep understanding of the nanoscopic system and its interaction with the environment. We report on experimental/theoretical results on controlling the spin degree of freedom of the color center nitrogen-vacancy in diamond and its nearby nuclear spin bath. We also report on current developments to study new color centers in diamond.					
15. SUBJECT TERMS color centers, nitrogen-vacancy, spin coherence					
16. SECURITY CLASSIFICATION OF:			17. LIMITATION OF ABSTRACT	18. NUMBER OF PAGES	19a. NAME OF RESPONSIBLE PERSON
a. REPORT	b. ABSTRACT	c. THIS PAGE			Jeronimo Maze
U	U	U	SAR	8	19b. TELEPHONE NUMBER (Include area code) 56-2-2354 4486

# FINAL PERFORMANCE REPORT

To: [technicalreports@afosr.af.mil](mailto:technicalreports@afosr.af.mil)

Subject: Final Performance Report to Dr. Brett Pokines

Contract/Grant Title: Engineering Electronic and Optical Properties of Color Centers in Diamond

Contract/Grant #: FA9550-12-1-0214

Reporting Period MAY, 01, 2012 to APR, 30, 2013

Annual accomplishments: see below

Archival publications (published) during reporting period: see below

Changes in research objectives, if any: None

Change in AFOSR program manager, if any: None

Extensions granted or milestones slipped, if any: None

Include any new discoveries, inventions, or patent disclosures during this reporting period (if none, report none): None

Other Identifying Information:

Recipient Organization: PONTIFICIA UNIVERSIDAD CATOLICA DE CHILE, AVENIDA VICUNA MACKENNA 4860, SANTIAGO 7820436, CHILE.

Recipient Principal Investigator: Dr. Jeronimo Maze, Physics Faculty, Pontificia Universidad Catolica, 011.56.2.2354.4486, [jmaze@uc.cl](mailto:jmaze@uc.cl)

DUNS: 980870054

Reporting Period End Date: JUL, 31, 2013

Govt Program Manager: Dr. Brett Pokines, AFOSR/IO, 011.56.2.330.3184, [brett.pokines@afosr.af.mil](mailto:brett.pokines@afosr.af.mil)

## 1. Abstract

We report on the results achieved during the period of the proposal as well as the current progress that will lead to results outside this period. The work of the proposal has concentrated on controlling the electronic, optical and spintronics properties of color centers in diamond and their environment. A high level of control of the before mentioned properties is crucial to develop novel applications such as single photon sources on demand, high precision and high resolution magnetic and electric sensors and opto-electronic devices at very low power consumption. All these applications require a deep understanding of the nanoscopic system and its interaction with the environment. In what follows, we report on experimental/theoretical results on controlling the spin degree of freedom of the color center nitrogen-vacancy in diamond and its nearby nuclear spin bath. We also report on current developments to study new color centers in diamond.

## 2. Accomplishments

### 2.1 Free Induction Decay in Diamond

We study, both theoretically and experimentally, the free induction decay (FID) of the electron spin associated with a single nitrogen-vacancy defect in high-purity diamond, where the main source of decoherence is the hyperfine interaction with a bath of  $^{13}\text{C}$  nuclear spins. In particular, we report a systematic study of the FID signal as a function of the strength of a magnetic field oriented along the symmetry axis of the defect. On average, an increment of the coherence time by a factor of  $\sqrt{5}/2$  is observed at high magnetic field in diamond samples with a natural abundance of  $^{13}\text{C}$  nuclear spins, in agreement with numerical simulations and theoretical studies. Further theoretical analysis shows that this enhancement is independent of the concentration of nuclear-spin impurities. By dividing the nuclear-spin bath into shells and cones, we theoretically identify the nuclear spins responsible for the observed dynamics.

See Appendix 1 for more information and Section 3 of this report.

### 2.2 Observing multiple quantum jumps of nuclear spin environment

We use the electronic spin of a single nitrogen-vacancy defect in diamond to observe the real-time evolution of neighboring single nuclear spins under ambient conditions. Using a diamond sample with a natural abundance of  $^{13}\text{C}$  isotopes, we first demonstrate high fidelity initialization and single-shot readout of an individual  $^{13}\text{C}$  nuclear spin. By including the intrinsic  $^{14}\text{N}$  nuclear spin of the nitrogen-vacancy defect in the quantum register, we then report the simultaneous observation of quantum jumps linked to both nuclear spin species, providing an efficient initialization of the two qubits. These results open up new avenues for diamond-based quantum information processing including active feedback in quantum error correction protocols and tests of quantum correlations with solid-state single spins at room temperature.

See Appendix 2 for more information and Section 3 of this Report.

## 3 Archival publications

1) J R Maze[1], A Dreau [2], V Waselowski [1], H Duarte [1], J-F Roch [3] and V Jacques [2]. “Free Induction Decay in Diamond”, New Journal of Physics 14, 103041 (2012).

Affiliations: [1] Departamento de Fisica Pontificia, Universidad Catolica de Chile, Santiago 7820436, Chile [2] Laboratoire de Photonique Quantique et Moleculaire, CNRS and ENS Cachan, UMR 8537, F-94235 Cachan, France. [3] Laboratoire Aime Cotton, CNRS, Universite Paris-Sud and ENS Cachan, F-91405 Orsay, France.

2) A. Dreau[1], P. Spinicelli[1], J. R. Maze[2], J.-F. Roch[3], and V. Jacques[1,3]. “Single-Shot Readout of Multiple Nuclear Spin Qubits in Diamond under Ambient Conditions”. Phys. Rev. Lett. 110, 060502 (2013).

Affiliations: [1] Laboratoire de Photonique Quantique et Moleculaire, Ecole Normale Supérieure de Cachan and CNRS UMR 8537, 94235 Cachan, France. [2] Facultad de Fisica, Pontificia Universidad Catolica de Chile, Santiago 7820436, Chile. [3] Laboratoire Aime Cotton, CNRS UPR 3321 and Universite Paris-Sud, 91405 Orsay, France

## **4. Undergoing research**

### **4.1 Implantation of new ions in diamond**

We are currently exploring the creation of new color centers in diamond. The results are being explored at the moment in our facilities. In addition, we are exploring the possibility of implanting gold nano-particles in the diamond matrix. This work has been in collaboration with Dr. Alejandro Reyes from UNAM, Mexico and Dr. Paras Prasad from Buffalo University.

### **4.2 Description of defect Silicon-Vacancy center in diamond**

Other color centers in diamond different than the nitrogen-vacancy center can have similar or better properties. We are currently investigating the electronic properties of silicon vacancy center in diamond. The results are partial and have not yet been published. The student Victor Waselowski (Pontificia Universidad Catolica) has been working on theoretical aspects together with experimentalists from University of Saarland (PhD Student Christian Hepp and Professor Christoph Becher) and University of Cambridge (Mete Atatüre). The Principal Investigator (Jeronimo Maze) has given two seminars related with these results:

“Modelling trapped electrons in defects in diamond and the effect of nuclear spin bath on their coherence time”, Workshop on Diamond - Spintronics, Photonics, Bio-applications, April 27-29, 2013, **Hong Kong**.

“Theoretical description for artificial atoms in diamond and the effect of nuclear spin bath on their coherence time”, Artificial Atoms: from Quantum Physics to Applications, 20-23 May 2013, Budapest, Hungary

## **5. Concluding remarks**

The one-year grant from AFOSR allowed us to achieve crucial steps toward engineering the spin, electric and optical properties of color centers in diamond. In a near future this support will allow us to continue our ongoing research and explore other nanosystems or color centers in large band gap materials. This will make key contributions toward realizing applications in quantum opto-electronics, single photon sources on demand, and high resolution and high sensitive sensors.

AFOSR support has been used not only to run our operational costs and acquire small equipment but also to support student's research. We look forward to future collaboration/agreements with Air Force Office of Scientific Research.

Jeronimo Maze  
Assistant Professor  
Faculty of Physics  
Pontificia Universidad Catolica de Chile

## Appendix

### A.1 Free Induction Decay in Diamond

Here we describe the findings of the results published in New Journal of Physics 14, 103041 (2012).

We consider an Atomic structure of the NV defect in diamond consisting of a substitutional nitrogen atom (N) associated with a vacancy (V) in an adjacent lattice site of the diamond matrix. The NV defect axis  $z$  provides an intrinsic quantization axis for the electron spin and a magnetic field  $B$  is applied along this axis (see Figure A1a and b).

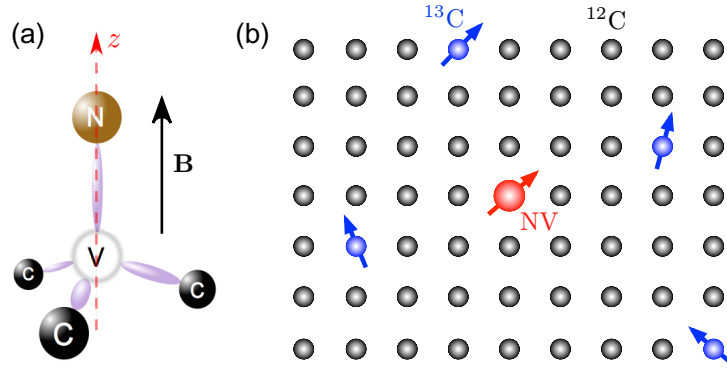


**Figure A1.** (a) Atomic structure of the NV defect in diamond. (b) Schematic view of a single NV defect (red arrow) placed in a nuclear-spin bath. Blue arrows indicate  $^{13}\text{C}$  nuclear spins located randomly in the diamond lattice. Decoherence of the central electronic spin is induced by hyperfine coupling with the  $^{13}\text{C}$  nuclear spins.

The experimental sequence used to measure the FID of the NV defect electron spin is shown on Figure A2a. A first laser pulse (2 $\mu\text{s}$ ) is used to polarize the electron spin in the  $m_s = 0$  sublevel. A Ramsey sequence consisting of two resonant microwave (MW)  $\pi/2$ -pulses separated by a variable free evolution duration  $\tau$  is then applied and a second laser pulse is finally used for spin-state read-out. For data analysis, the NV defect PL recorded during the first 300 ns of the laser pulses is used for spin-state read-out while the PL recorded during the last 300 ns is used as the reference. See Figure A2b for typical recorded FID signals and Figure A2c for simulations.

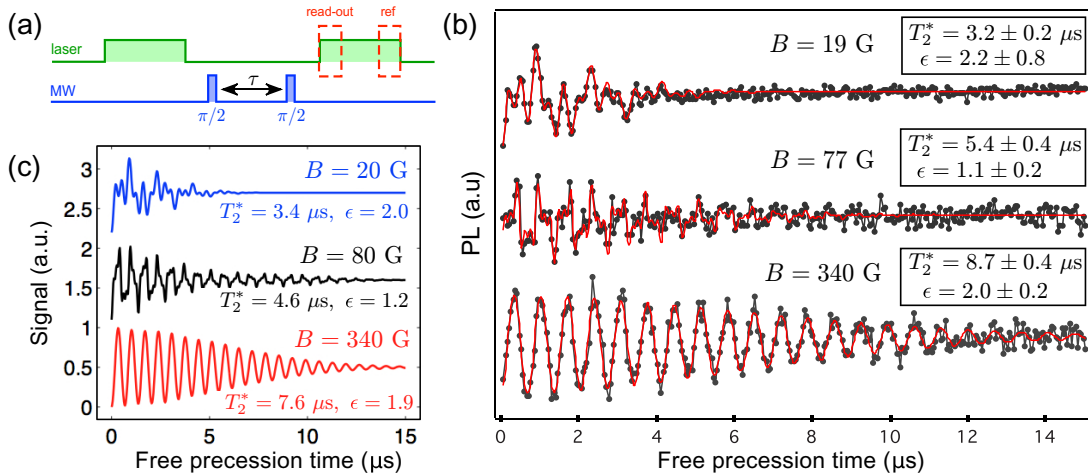


**Figure A2.** (a) Experimental sequence used to measure the FID. of the NV defect electron spin. (b) Typical FID signals recorded from a single NV defect (NV12) for three different magnetic field amplitudes applied along the NV defect axis. The red solid line is data fitting as explained in the main text. (c) Numerical simulations of the FID signal for a particular  $^{13}\text{C}$  distribution. These graphs are obtained by multiplying the simulated FID envelope by the magnetic field-dependent populations of each  $^{14}\text{N}$  nuclear-spin state. *Figure from New Journal of Physics 14, 103041 (2012).*

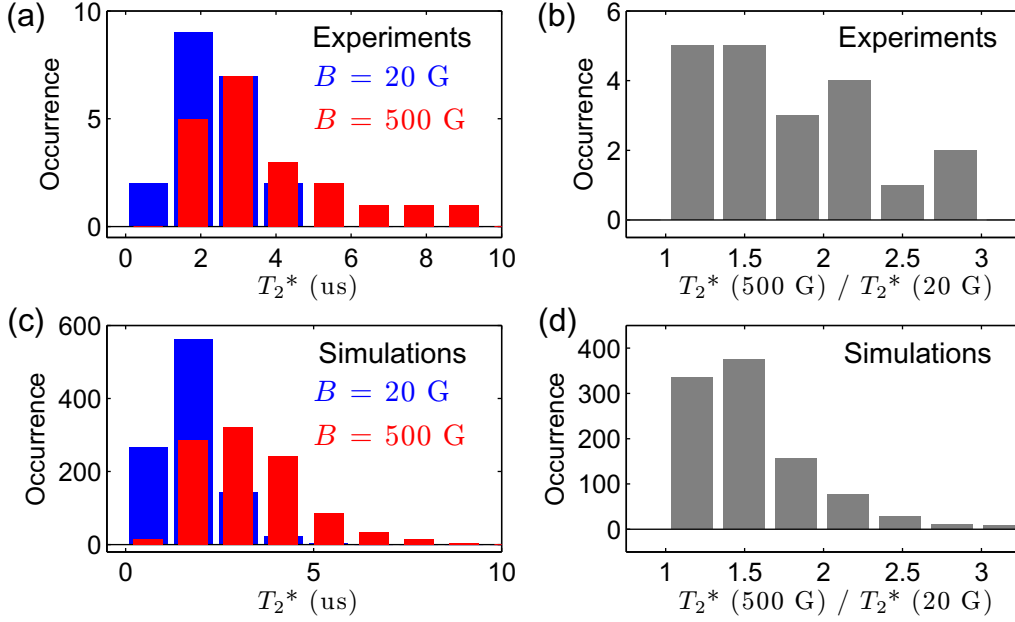


**Figure A3.** (a) Experimental and (c) theoretical histograms of the coherence time  $T_2^*$  over 20 and 1000 different  $^{13}\text{C}$  bath configurations, respectively. (b) Corresponding experimental and (d) theoretical distributions of the coherence time enhancement between weak magnetic field ( $B = 20$  G) and high magnetic field ( $B = 500$  G). *Figure from New Journal of Physics 14, 103041 (2012).*

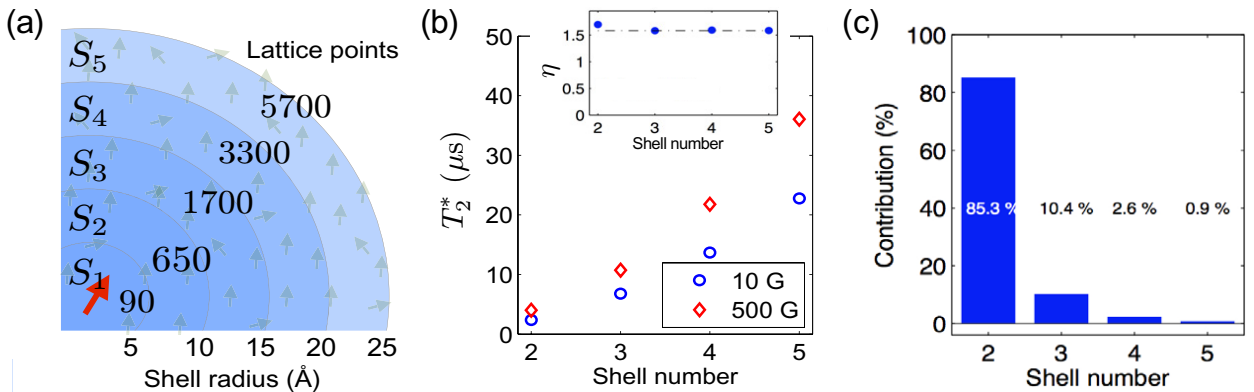


**Figure A4.** (a) Shell partition of the nuclear-spin bath. Each shell  $S_i$  has a thickness of  $5 \text{ \AA}$ . The number of lattice points per shell is indicated. (b) Coherence time versus shell number for low (10G) and high (500G) magnetic fields. The calculation is performed with the numerical method N2 for a natural abundance of  $^{13}\text{C}$ . The coherence time enhancement for each shell is

equal to  $\sqrt{5}/2$ , as shown in the inset. (c) Contribution of each shell to decoherence calculated as  $(T^*/T^*_{\text{shell}})^2$ . As expected, nuclei close to the central spin contribute the most. *Figure from New Journal of Physics 14, 103041 (2012).*

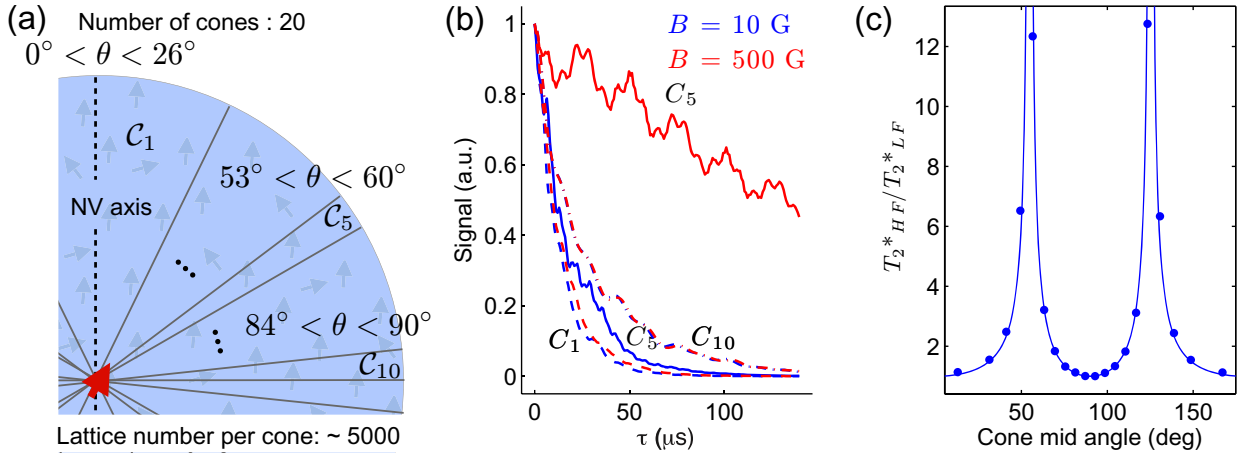


**Figure A5.** (a) Cone partition of the nuclear-spin bath. Each cone contains approximately the same number of lattice sites ( $\sim 5000$ ). Cones  $C_1$ ,  $C_5$  and  $C_{10}$  contain nuclear spin close to the north pole, to the magic angle  $\theta_M \approx 54^\circ$ , and to the equator, respectively. (b) Envelope of the FID signal for cones  $C_1$  (dashed lines),  $C_5$  (solid lines) and  $C_{10}$  (dashed-dot lines) at weak magnetic field (blue) and at high magnetic field (red). (c) Coherence time enhancement factor  $\eta$  as a function of the cone mid-angle. The maximum enhancement occurs for nuclei with a polar angle  $\theta$  close to the magic angle. *Figure from New Journal of Physics 14, 103041 (2012).*

## Conclusions

We observe an enhancement of the coherence time for high magnetic fields. This behavior can favor applications such as magnetic sensing by suppressing decoherence and therefore increasing the maximum sensitivity. Not all color centers have the same response to the external magnetic field. We observe this behavior depends on the number of impurities close to the magic angle and the effective concentration of spin impurities. Understanding this behavior can be useful for characterizing the environment of color centers and achieve total control of the electronic spin and perhaps nearby nuclear spins for quantum information applications.

## A.2 Observing multiple quantum jumps of nuclear spin environment

Here we describe the main findings of the result published in Phys. Rev. Lett. 110, 060502 (2013).

Consider a nitrogen-vacancy defect in a high purity sample diamond with low concentration of electronic impurities. See Figure A6 for the energy level diagram.

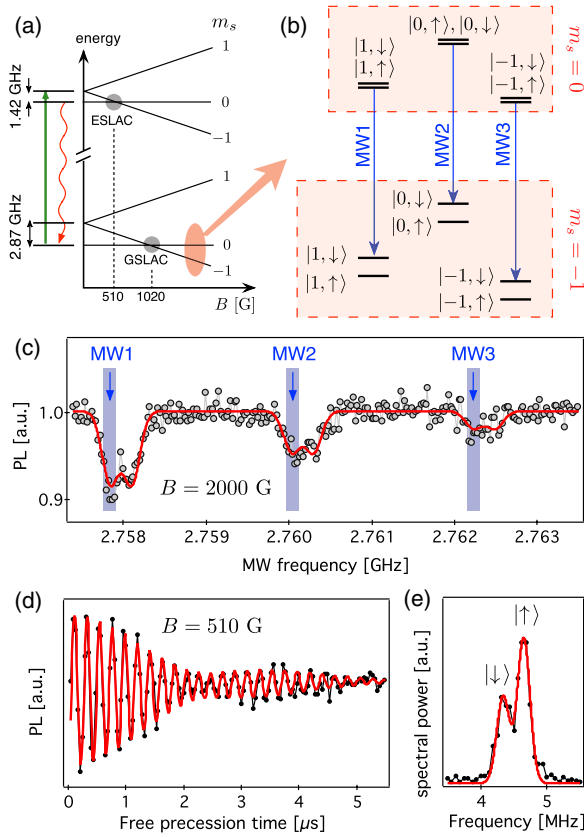


**Figure A6.** (a) Energy-level diagram of the NV defect as a function of the strength of a static magnetic field  $B$  applied along the NV defect axis. Level anticrossings in the ground state and in the excited state are highlighted. (b) Hyperfine structure of the  $m_s = 0$  and  $m_s = -1$  electron spin manifolds for a NV defect coupled with its intrinsic  $^{14}\text{N}$  nuclear spin ( $|m_I\rangle$ ) and with a nearby single  $^{13}\text{C}$  nuclear spin (up or down). The hyperfine sub-levels are denoted as  $|m_I, \uparrow\rangle$ ,  $|m_I, \downarrow\rangle$ . Blue arrows indicate the microwave (MW) transitions used for single-shot readout measurements. (c) Optically detected ESR spectrum recorded for a magnetic field  $B = 2000$  G. (d) FID signal of the NV defect electron spin recorded at the ESLAC ( $B = 510$  G) showing a coherence time  $T_2 = 2.9 \pm 0.1$  us. (e) Fourier transform of the FID signal. *Figure from Phys. Rev. Lett. 110, 060502 (2013).*

Single shot readout sequence is shown on Figure A7. The read-out sequence uses three microwaves to be insensitive to the different states of the nitrogen nuclear spin.

By using only one microwave, the quantum jumps of the nitrogen nuclear spins are revealed on a time scale much shorter than the quantum jumps of the nearby  $^{13}\text{C}$ . See Figure A8.



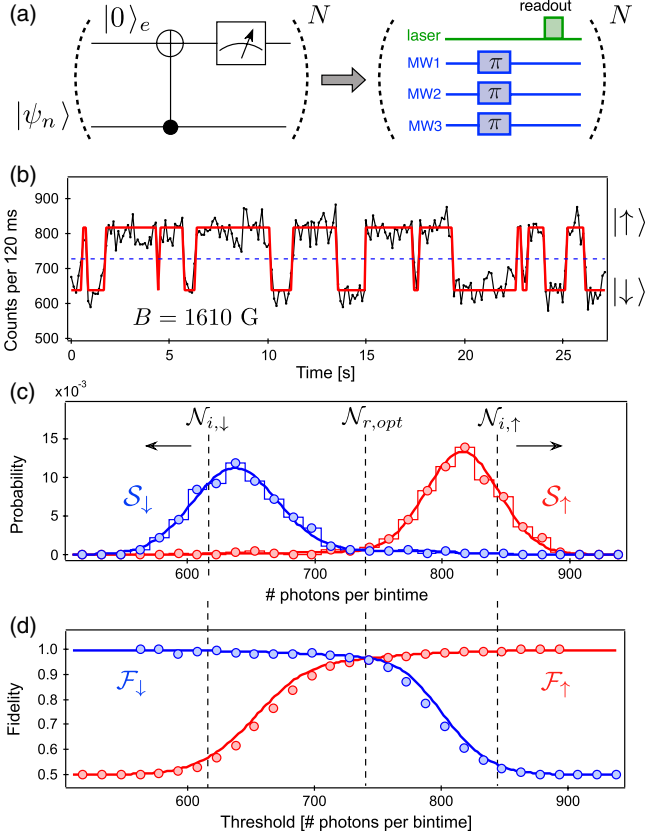


**Figure A7.** (a) Logic diagram of the single-shot readout scheme and corresponding experimental sequence. The duration of the pi-pulses is set to 4  $\mu$ s. The 300 ns laser pulse is used both for spin-state read-out and to achieve an efficient preparation of the NV defect electron spin in the  $m_s = 0$  sub-level at each repetition of the sequence. (b) PL time trace showing quantum jumps of the  $^{13}\text{C}$  nuclear spin state. The solid line is a fit with a two states hidden Markov model from which the relaxation time  $T_1$  of the nuclear spin state is extracted. (c) Normalized nuclear-spin dependent photon counting distributions  $S$ . The solid lines are data fittings.

(d) Single-shot readout fidelity  $F$  as a function of the readout threshold. The initialization thresholds  $N_i$  and the optimized discrimination threshold  $N_{r,opt}$  are indicated with dashed lines. The solid lines are extracted from the fits in (c). The initialization fidelity in state up(down) is

given by  $F_{up}$  ( $F_{down}$ ). *Figure from Phys. Rev. Lett. 110, 060502 (2013).*

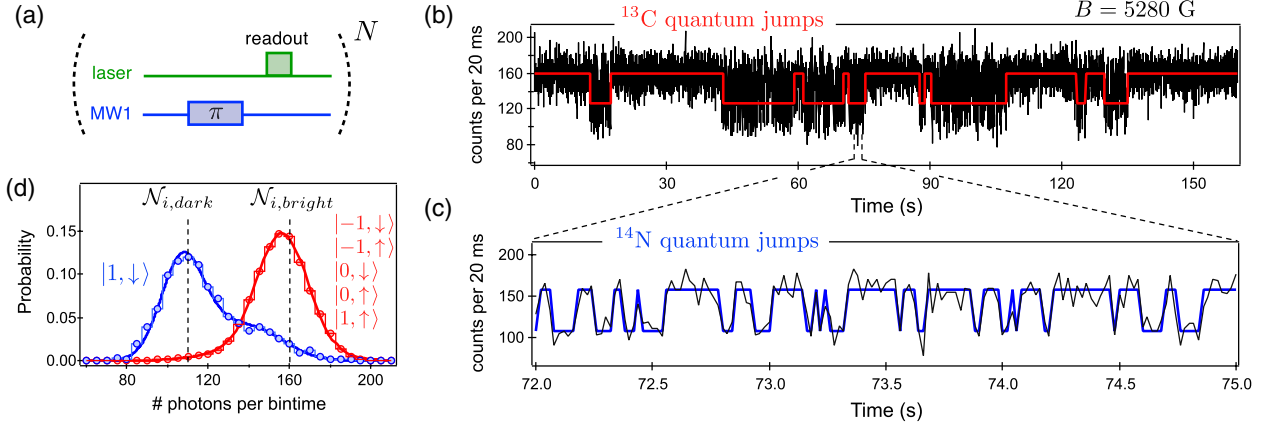


**Figure A8.** (a) Experimental sequence. (b), (c) PL time trace recorded by continuously repeating the sequence for a magnetic field  $B = 5280$  G. Each data point corresponds to approximately 3000 repetitions of the readout sequence (20 ms). Quantum jumps linked to (b) the weakly coupled  $^{13}\text{C}$  nuclear spin and to (c) the intrinsic  $^{14}\text{N}$  nuclear spin can be distinguished. (d) Normalized nuclear-spin dependent photon counting distributions measured with the initialization thresholds set to  $N_{i,dark} = 110$  counts and  $N_{i,bright} = 160$  counts. The projective readout fidelity is optimized for a discrimination threshold  $N_{r,opt} = 135$  counts. *Figure from Phys. Rev. Lett. 110, 060502 (2013).*

These results open the door for future applications in quantum information involving several quantum bits.